A Small-Angle Neutron Scattering Investigation of the Configuration of Poly(*p*-phenylene) Precursors in Solution

J. R. Holland and R. W. Richards*

Interdisciplinary Research Centre in Polymer Science and Technology, University of Durham, Durham DH1 3LE, UK

A. N. Burgess and A. Nevin

ICI Chemicals and Polymers Ltd., The Heath, Runcorn WA7 4QE, UK

Received March 30, 1995; Revised Manuscript Received September 11, 1995®

ABSTRACT: Small-angle neutron scattering (SANS) has been used to investigate the configuration of partially aromatized precursor polymers of poly(*p*-phenylene) in *N*-methylpyrrolidinone solution. The range of aromatization covered was 0–80%, and a number of precursor polymer molecular weights were used. Although the aromatization process is accompanied by degradation and aggregation, it has been possible to interpret the SANS data using scattering laws for stiff chains. From this analysis, persistence lengths and shift factors have been obtained for aromatizations up to 40%; persistance lengths range from 22 to 32 Å and shift factors from an average of 40 to 20 $Å^{-1}$. Above this degree of aromatization there is a distinct change in the SANS profile. When these data are plotted in Kratky format, a distinct maximum was observed. For aromatizations greater than 40%, the configuration in solution has been interpreted as the formation of starlike aggregates where insoluble polyphenylene cores are maintained in solution by solvated unaromatized portions of the aggregate which form the arms of the star. As aromatization increased from 50% to ~80%, the radius of gyration of three different molecular weight fractions varied little but the number of arms increased. The suitability of the polydisperse star model for the highest percentage aromatization is questionable, and possible alternatives are discussed. The complications of degradation and increase in polydispersity prevent the use of more complex models. Aromatization does not lead to any significant increase in rodlike configuration of the molecules. The dominant effect is aggregation to form clusters that have starlike characteristics.

Introduction

Poly(*p*-phenylene) (PPP) is one of several polymers with a high concentration of aromatic groups in the main-chain backbone that have been investigated as electroluminescent materials, particularly for the emission of light in the blue region of the visible spectrum.[1-3] The polymer is also susceptible to conductivity changes by doping processes, and the intrinsic linearity of the molecule should result in high mechanical strength at least in the direction of the chain axis. These attractive properties of the polymer are countered by the failure (thus far) to synthesize a high molecular weight polymer. Early attempts at the synthesis were alluded to by us in a preceding paper.[4] Perhaps the most innovative approach has been that of Ballard et al.,[5] who used a biological route to prepare a substituted cyclohexadiene which could be polymerized and then subsequently converted to PPP by a pyrolysis procedure.

The pyrolysis step is base catalyzed and can be relatively easily performed in *N*-methylpyrrolidinone solution; however, full aromatization of the precursor, whether in solution or solid state, leads to oligomeric PPP and the causes of such degradation have been speculated on and discussed.[4,6] In our earlier papers, we described the application of size exclusion chromatography (SEC) to follow the aromatization process[4] and the use of dilute solution viscometry and light scattering to establish the configurational changes.[7] SEC data showed that the molecular weight distribution rapidly became bimodal on aromatization of the precursor polymer, and it was suggested that this was due to the occurrence of long sequences of phenylene units which were insoluble in the solvent. Such long sequences aggregate intermolecularly and produce the high molecular weight fraction observed.

In principle, it is anticipated that PPP should have a linear rodlike configuration due to the main-chain backbone consisting of phenylene units. Configurational changes in the early stages of aromatization (up to ~20%) have been investigated using dilute solution viscometry and light scattering.[7] Interpretation of these data was made using the wormlike chain model of semiflexible polymers first introduced by Kratky and Porod.[8] This model is describable by two factors, the persistence length (a) and the contour length (L; or shift factor M_L). An increase in the persistence length indicates a "stiffening" or straightening of the polymer molecule. We discuss here the application of small-angle neutron scattering (SANS) in the evaluation of the configuration of partially aromatized precursor polymers of PPP. In addition to reporting results for aromatizations less than 40%, we also discuss the nature of the species for aromatizations approaching 80% where aggregation plays a much more important role.

Theory

The wormlike chain model was first introduced by Kratky and Porod and utilizes the concept of a persistence length, a. This is the average length of the end-to-end vector projected on the direction of the first bond in the molecule, thus for N bonds of length l

$$a = \lim_{Nl\to\infty} \frac{l}{1 + \cos\theta} \tag{1}$$

where θ is the bond angle.

* To whom correspondence should be addressed.
® Abstract published in *Advance ACS Abstracts,* October 15, 1995.

0024-9297/95/2228-8167$09.00/0

For molecules of finite size, the wormlike chain is obtained by reduction of the bond length to zero with a parallel increase of the number of segments to keep the contour length (L) constant. At the same time, the bond angle is enlarged so that the persistence length retains a finite value. This results in a continuously curving chain where there are random changes of curvature from point to point.[9] The mean square radius of gyration, $\langle s^2 \rangle$, for the wormlike chain was derived by Benoit and Doty[10] as

$$\langle s^2 \rangle = \frac{aL}{3} - aL^2 + \frac{2a^3}{L} - \frac{2a^4}{L^2}(1 - \exp(-L/a)) \quad (2)$$

Due to the large range of scattering vector ($Q = (4\pi/\lambda) \sin\theta$ with λ the radiation wavelength in the scattering medium and 2θ the scattering angle) accessible to SANS, the particle scattering factor, $P(Q)$, for a polymer molecule can be examined for a length-scale range from the global dimensions of the molecule down to distances of about one monomer unit in length. For flexible polymer molecules, the Debye scattering law provides a good description of the observed scattering. However, at larger values of Q beyond the Guinier regime ($Q\langle s^2 \rangle^{1/2} \geq 1$), the Debye equation fails to account for the short length scales behaving as an assembly of randomly oriented thin rods. Neugebauer[11] derived the scattering law for thin rods some 50 years ago. The conversion of the precursor cyclohexadiene polymer to PPP is anticipated to be accompanied by a change from a Gaussian coil configuration to that of a linear rigid rod, and thus a particle scattering function able to incorporate flexible chain and rigid chain behavior in varying proportions is desired. It is for this reason that the wormlike chain is attractive since increasing the persistence length introduces a more rodlike nature to the model, and in the limit of a/L approaching zero a flexible coil configuration is regained.

Since the original definition of the Kratky–Porod wormlike chain, there have been several attempts at calculating the particle scattering function for such a model. Monte Carlo calculations have been reported by Heine et al.[12] and Kirste,[13] but such methods are not particularly amenable for practical use. Analytical expressions[14,15] were obtained before the Monte Carlo results, and these were utilized by Burchard and Kajiwara[16] to produce a distribution function for a real discrete chain and an approximation to the particle scattering function obtained.

Perhaps the most detailed consideration of stiff chain polymers has been that of Yamakawa and coworkers.[17–22] Whereas the original wormlike chain can be likened to an elastic wire whose bending force constant, κ_0 is given by

$$\kappa_0 = k_B T a \quad (3)$$

the *helical* wormlike chain model developed by Yamakawa includes torsional energy as well. In addition to the bending and torsional force constants, two other parameters are required, the helix pitch and helix diameter, to describe this model completely. Yoshizaki and Yamakawa[21] have developed this model to obtain the isotropic particle scattering function for helical wormlike chains written in terms of Q and contour length. From the viewpoint of differentiating between the configurational models, scattering data are best plotted as Kratky plots, i.e., $Q^2I(Q)$ as a function of Q, and the expressions obtained by Yoshizaki and Yamakawa are written directly in this manner; i.e., they derive a function $F(Q,L)$ which is $LQ^2P(Q,L)$ and

$$F(Q,L) = F_0(Q,L)\Gamma(Q,L) \quad (4)$$

where

$$F_0(Q,L) = (1 - \chi(Q,L))F_D(Q,L) + \chi(Q,L)F_R(Q,L) \quad (5)$$

In eq 5, $F_D(Q,L)$ is the Debye scattering law[23] for a flexible random coil (written in Kratky plot format),

$$F_D(Q,L) = (2Q^2L/u^2)(\exp(-u) + u - 1) \quad (6)$$

with $u = \langle s^2 \rangle Q^2$. The function $F_R(Q,L)$ is the equivalent scattering law for a rod:[11]

$$F_r(Q,L) = 2Q\,\mathrm{Si}(QL) - \frac{4}{L}\sin^2(QL/2) \quad (7)$$

where $\mathrm{Si}(x)$ is the sine integral. The factor $\chi(Q,L)$ in eq 5 is given by

$$\chi = \exp(-(\pi\langle s^2 \rangle Q/2L)^{-5}) \quad (8)$$

and $\Gamma(Q,L)$ in eq 4 is a sum of additive factors which also involve χ. The value of the parameters involved in $\Gamma(Q,L)$ (in addition to χ) depend on the nature of the helical wormlike chain, i.e., whether it is a simple Kratky–Porod chain or a true helical chain, in which case the helix radius and pitch parameters play a role in defining the parameters in $\Gamma(Q,L)$. A series of values of these parameters have been tabulated by Yoshizaki and Yamakawa.[21]

In these equations, the mean square radius of gyration is that of the helical wormlike chain being considered; thus for a Kratky–Porod chain, this is given by eq 2. An additional factor is that all of the equations are couched in length scales whose units are $2a$, i.e., twice the persistence length; thus the scattering vector is dimensionless. Figure 1 shows the form of the Kratky plots anticipated for Kratky–Porod wormlike chains. In the low-Q region (Guinier region), the curves are coincident with that for a random coil with the radius of gyration of the Kratky–Porod chain (eq 2). For Q values greater than the Guinier range, the wormlike chain departs from the scattering of the random coil and asymptotically approaches that for a rodlike molecule. In the limit of very high Q, the scattering from a rod, the helical wormlike chain, and the Kratky–Porod wormlike chain are all coincident. At the other extreme, i.e., very low Q, the scatterings for the different wormlike chains are all coincident with that for a flexible random coil model.

Evidently, the helical wormlike chain model is able to describe a range of configurational flexibility; a notable feature is that, as derived by Yoshizaki and Yamakawa, the particle scattering function for the Kratky–Porod wormlike chain seems not to possess a large region of Q where the ordinate has a plateau. A plateau region has often been observed in the small-angle scattering from polymers and is predicted by other derivations of the particle scattering function (e.g., that due to Koyama).[24] The occurrence of a plateau in other derivations for the particle scattering function has been attributed to the approximations made in those other approaches.

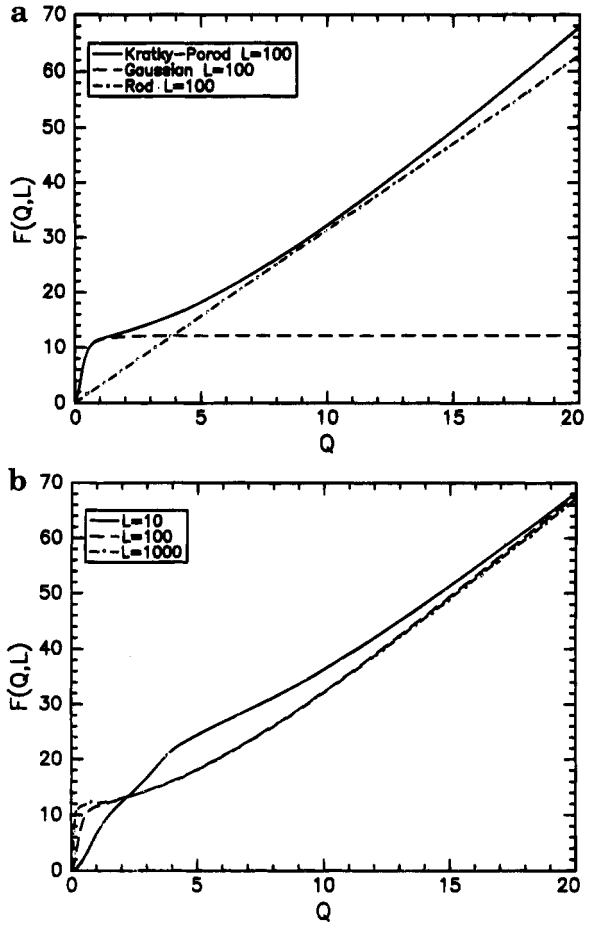

Figure 1. (a) Scattering of a Kratky–Porod molecule (solid line) calculated from the equation due to Yoshizaki and Yamakawa (eq 4). All lengths are in units of a, thus L = (contour length/a) and Q = (a/scattering vector). Dashed line is the scattering from a Gaussian coil, and the chain line is the scattering from a rodlike molecule each having the same contour length as the Kratky–Porod chain. (b) Variation in the parameter $F(Q,L)$ for a Kratky–Porod molecule as a function of the dimensionless contour length, L.

The Koyama expression for the particle scattering function of a stiff chain is

$$P(Q,L) = \frac{1}{L^2}\int_0^L (L-x)\exp\left[\frac{-S^2 x f(x)}{3}\right]\frac{\sin(Sxg(x))}{Sxg(x)}\,dx \tag{9}$$

with $S = Qa$ and $x = at$, where t is the contour length of a partial chain segment and the contour length is a dimensionless form in units of the persistence length, a. In eq 9,

$$x^2 g(x)^2 = a\langle r^2\rangle\sqrt{10}\left\{1 - \frac{0.6\langle r^4\rangle}{\langle r^2\rangle^2}\right\}^{1/2} \tag{10}$$

$$xf(x) = a^2\langle r\rangle^2 - \frac{x^2 g(x)^2}{2} \tag{11}$$

where $\langle r^2\rangle$ and $\langle r^4\rangle$ are the second and fourth moments of the distribution of the end-to-end distance of the molecule.

Although the helical wormlike chain is the much more flexible model, the number of parameters (five) to be determined in defining it make it impractical to attempt to fit this model to scattering data. We use only two models here in the analysis of our SANS data on the partially aromatized precursors to PPP. They are the Kratky–Porod wormlike chain with the particle scattering function as derived by Yoshizaki and Yamakawa[21] (eq 4), and the expression due to Koyama[24] (eq 9) for the same chain model.

Table 1. Molecular Weight and Polydispersity of Deuterated Precursor Polymer

fraction	$\bar{M}_w/10^6$ g mol^{-1}	$\bar{M}_w/\bar{M}_n$	fraction	$\bar{M}_w/10^6$ g mol^{-1}	$\bar{M}_w/\bar{M}_n$
A	1.208	1.64	E	0.202	1.43
B	0.628	1.48	F	0.100	1.53
C	0.409	1.42	G	0.050	1.84
D	0.350	1.22	H	0.020	1.25

Experimental Section

Polymer Synthesis and Fractionation. The free radical polymerization of the hydrogenous precursor monomer and the subsequent fractionation and pyrolysis of the precursor polymer have been described previously.[4] For the preparation of deuterated polymer, the same procedure was used except that the monomer, 5,6-*cis*-dimethylcarboxycyclohexia-1,3-diene (DHCDDMC-*d*; **1**) was fully deuterated.

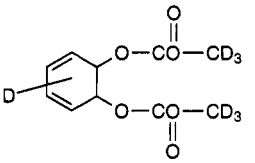

1

The degree of conversion of **1** to polymer was 65.6%, and it was noted that the molecular weight of the deuterio polymer was higher than that of the hydrogenous polymer prepared under identical conditions of initiator concentration and temperature, presumably due to a lower incidence of chain transfer via deuteron abstraction in the polymerization of the deuterio polymer. From this polymer, eight fractions were obtained and the molecular weights and polydispersities obtained by size exclusion chromatography are given in Table 1.

Aromatization to various extents was carried out by heating *N*-methylpyrrolidinone (NMP) solutions at 448 K for defined times. The polymer was then precipitated from these solutions, filtered, washed, and dried at 313 K to constant weight. After drying, the partially aromatized fractions were stored in a freezer. To ensure that no deuterium exchange had taken place, the precursor polymer and the partially aromatized polymer were analyzed by ^{1}H NMR using a 400-MHz instrument. From comparisons of spectra in deuteriochloroform solution and in a solution doped with a known amount of trichloroethylene, it was concluded that the precursor polymer was 99.5% deuterated and the partially aromatized polymer in excess of 99% deuterated. This NMR analysis was also repeated on samples after the SANS experiments; the results confirmed there had been no change in the level of deuteration.

Small-Angle Neutron Scattering. SANS experiments were made on the precursor polymer and partially aromatized polymer solutions in NMP. Two series of experiments were undertaken at a temperature of 298 K. In the first of these, a series of solutions with a polymer concentration between 2 and 5% (w/v) were made from four fractions (A, B, C, E) of poly(DHCDDMC-*d*). Two of these fractions were also aromatized to two different extents of aromatization and again a series of solutions in NMP made covering the same concentration range as the precursor polymers. The SANS data for each of these solutions were obtained using the D17 diffractometer at the Institut Lane-Langevin, Grenoble, France. In each case, the solution was contained in quartz cells with a path length of 1 mm, the incident neutron beam had a wavelength of 12 Å with a wavelength distribution of 10%, the sample to detector distance was set so that the range of scattering vector, Q, was

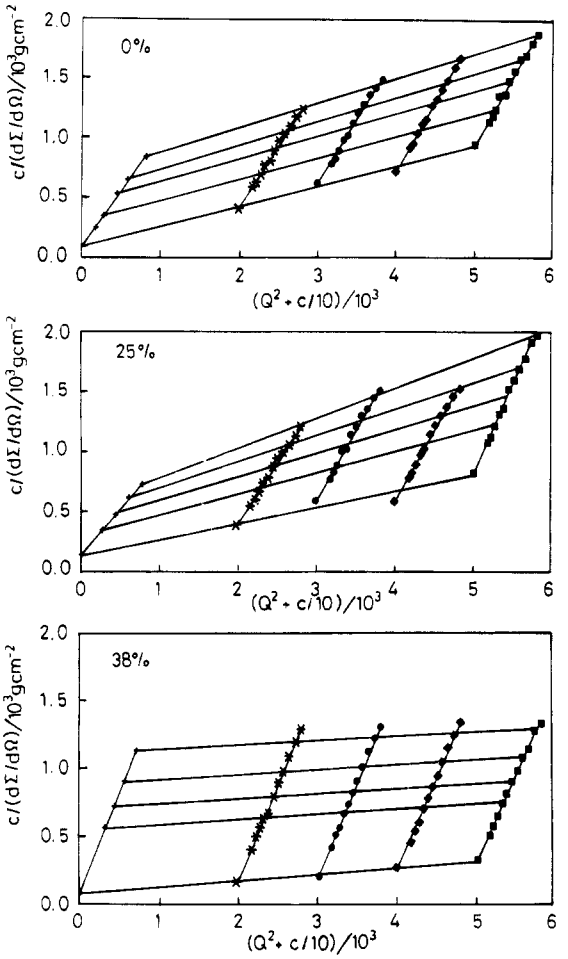

Figure 2. Zimm plots of SANS data for fraction E at 0, 25, and 38% aromatization.

from 6.6×10^{-3} to 9.5×10^{-2} Å^{-1}. Each data set was normalized and corrected to absolute cross sections using the scattering from a 1-mm-thick specimen of water. The background scattering due to the solvent was obtained separately and subtracted from the scattered intensities of the solutions. For each polymer, the SANS data from the solutions of different concentration were collected together in the form of Zimm plots and extrapolations to $Q = 0$ and $c = 0$ were made in the usual way.

In the second series of experiments, a single concentration (5% w/v) of each of four fractions (D, F, G, H) was used. Each fraction was aromatized to various extents between 0 and 80% in NMP solution. For percentage aromatizations below 40%, the polymer was precipitated from solution and redissolved in fresh NMP for the SANS experiments. For the higher percentage aromatizations, other work had shown that the precipitated polymer did not redissolve fully; indeed for the highest aromatization attained in solution (80%), a gel is formed. Therefore, for these samples, SANS experiments were carried out on the specimens as made with no precipitation and redissolution steps. SANS data were collected using the LOQ diffractometer at the UK pulsed neutron source, ISIS at the Rutherford Appleton Laboratory, Oxfordshire, UK. As in the D17 experiments, all samples were contained in quartz cells with a 1-mm path length. The range of scattering vector was much wider, being $1 \times 10^{-2} \leq Q/\text{Å}^{-1} \leq 0.2$, background scattering from the NMP solvent was subtracted, and the data were converted to absolute cross sections using the scattering from a well-characterized blend of deuteriopolystyrene in hydrogenous polystyrene as calibrant.

Results

Zimm Plots. Figure 2 shows the Zimm plots obtained for one fraction at different percentage aromatizations. From extrapolation of these data to $Q = 0$, $c = 0$ for all the polymers investigated in this way, the weight-average molecular weight, mean square radius of gyration, and second viral coefficient were obtained; these values are given in Table 2. Figure 3 shows a double-logarithmic plot of the weight-average mean square radius of gyration as a function of weight-average molecular weight for the unaromatized polymer. The weight-average values of the radii of gyration were obtained using the relation[25]

$$\langle s^2 \rangle_w = \langle s^2 \rangle_z \frac{(h+1)}{h+2}$$

and

$$h = \left(\frac{\bar{M}_w}{\bar{M}_n} - 1 \right)^{-1}$$

Included in Figure 3 are data obtained by light scattering from dilute solutions of hydrogenous poly(DHCDDMC). Although the data for these four deuterated fractions are of the same order of magnitude as those obtained by light scattering, it is evident that the SANS data give a lower radius of gyration for an equivalent molecular weight. It is not clear why this should be so; however, the values of the second viral coefficient obtained for the deuterio polymer in NMP are considerably smaller than those obtained by light scattering for the hydrogenous polymer. The relation between A_2 and $\bar{M}_w$ for the deuterio polymer obtained from SANS is

$$A_2 = (2.8 \times 10^{-2}) M_w^{-0.27}$$

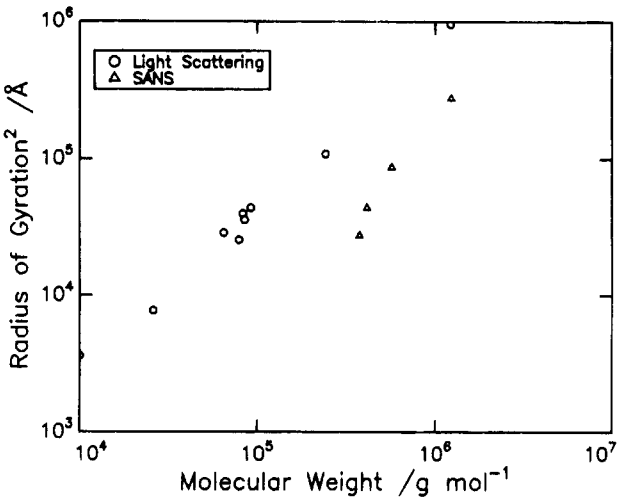

Figure 3. Double-logarithmic plot of the mean square radius of gyration obtained by light scattering and SANS for PPP precursors with 0% aromatization dissolved in NMP.

Table 2. Molecular Weights, Mean Square Radii of Gyration, and Second Viral Coefficients from SANS on NMP Solutions

fraction	% aromatzn	$\bar{M}_w/10^3$ g mol^{-1}	$\langle s^2 \rangle_z/10^4$ Å^{-2}	$A_2/10^{-4}$ cm^3 g^{-1} mol^{-1}
A	0	1230	38.44	6.5
B	0	571	11.56	7.9
C	0	415	3.60	8.4
C	28	218	1.70	6.5
C	38	495	6.76	2.6
E	0	377	2.76	9.2
E	13	346	2.89	7.6
E	25	281	1.96	10.3

Table 3. Mean Square Radii of Gyration and Molecular Weights of Partially Aromatized Polymer from LOQ Data[a]

		% aromatization							
fraction		0	10	20	30	40	50	60	80
H	$\bar{M}_w/10^3$	24	23	23	54		270	1300	20 000
	$\langle s^2\rangle/10^3$ Å^2	4.9	5.5	4.8	44.5				
G	$\bar{M}_w/10^3$	44	41	90	75		370	870	26 000
	$\langle s^2\rangle/10^3$ Å^2	14.4	11.7	46.7	71.8				
F	$\bar{M}_w/10^3$								
	$\langle s^2\rangle/10^3$ Å^2	32.4	15.9	16.9	34.2				
D	$\bar{M}_w/10^3$								
	$\langle s^2\rangle/10^3$ Å^2	109.0	12.5	13.5	28.6	65.0			

[a] Molecular weights from light scattering in dilute solution for 0% aromatization are (D) 350 000, (F) 100 000, (G) 50 000, and (H) 20 000 g mol^{-1}.

compared to

$$A_2 = (8.6 \times 10^{-3})\bar{M}_w^{-0.16}$$

for the hydrogenous polymer. Consequently, NMP is not as good a solvent for the deuterio polymer and the molecules will not be expanded as much as the hydrogenous polymer. However, three factors should be borne in mind. First, the SANS data are obtained from solutions of considerably higher concentration than those used for light scattering. This is to ensure that a good signal-to-noise ratio is obtained in a reasonable time. Second, only a narrow range of molecular weights has been investigated using SANS. Third, we note from the values of radius of gyration set out in Table 2 for fractions A and B that the product $Q\langle s^2\rangle_z^{1/2} > 1$, and this is outside the Guinier range within which values of the radius of gyration can be obtained. Even with the relaxation of this condition for polydisperse polymers as set out by Ullman,[26] the Q range is rather too large for fractions A and B. Consequently, the values of the radii of gyration and second virial coefficient obtained may not be the true values. However, we point out that the molecular weights obtained from the SANS data on these two polymers is in excellent agreement with those obtained by light scattering from dilute solutions.

Notwithstanding this apparent difference in behavior of the precursor polymer, the general influence of aromatization on the polymer observed in the SANS-obtained molecular weight is the same as that derived by us using size exclusion chromatography and light scattering on the hydrogenous polymer; i.e., a reduction in molecular weight is observed for aromatization up to ~25–30% and thereafter an increase in molecular weight is noted. This behavior in $\bar{M}_w$ is observed for fraction C as the aromatization changes from 0 to 38%. For fraction E, no increase in molecular weight was observed because aromatization was stopped at 25%. The mean square radii of gyration variation with aromatization also shows this trend; i.e., an initial decrease is followed by an increase at the highest percentage aromatization used.

A wider range of aromatizations for a series of four fractions (D, F, G, H) was investigated using the LOQ diffractometer. For aromatization up to 40%, these data were fitted over the whole Q range using the Debye expression with $\langle s^2\rangle_z$ and the intercept at $Q = 0$ as adjustable fitting parameters. We point out here that the Debye expression is the *simplest* expression we can use to obtain values for molecular parameters that will provide the basis for comparison in the first instance. A more detailed insight into the molecular configuration is provided in the Discussion section, where more complex models are applied. In principle, the molecular weight of the polymer is obtainable from the $Q = 0$ intercept; however, extraction of the molecular weight has only been done for the two fractions of lower molecular weight (G, H). Fractions D and F have much higher molecular weights, and an accurate value of the $Q = 0$ intercept is only obtainable if a sufficient range of Q where $Q\langle s^2\rangle^{1/2} \leq 1$ ($\cong$2 for polydisperse polymers) is sampled. The Q range of LOQ is such that there are insufficient data points at low Q to enable an accurate extrapolation for fractions D and F. By contrast, the value of $\langle s^2\rangle_z$ is not so dependent on this low-Q region provided the full Debye equation is used to fit the whole data curve, Table 3 gives the z-average mean square radius of gyration and molecular weights obtained (where accessible). The molecular weights given for percentage aromatizations greater than 40% should be treated with caution. Figure 4 shows selected SANS data and the Debye fits to these data. For these higher percentages of aromatization, the scattered intensity for $Q < 0.05$ Å^{-1} increases very rapidly; hence the intercept at $Q = 0$ is subject to a large uncertainty. For fractions G and H, the molecular weights up to an aromatization of 30% are acceptable because the low Q scattering cross sections do not increase rapidly. In obtaining these molecular weights, the scattering length density of the partially aromatized polymer has been calculated as the weighted sum of the scattering length density of the fully aromatized polymer and that for the unaromatized polymer. The molecular weights and the radii of gyration obtained show the same trends as the values obtained using D17 data, i.e., a decrease to a minimum value followed by an increase. This increase in molecular weight appears to continue as the aromatization proceeds further, although we emphasize again that the molecular weights for aromatizations greater than 40% are not to be taken as accurate values. For the two lowest molecular weight fractions (G, H), the decrease in molecular weight and radius of gyration are barely perceptible. However, for fractions D and F, there is a large decrease in mean square radius of gyration as soon as aromatization occurs. The radius of gyration falls to a value commensurate with a molecular weight of ~40 000 for an aromatization of 20%. When the percentage aromatization increases above this value, a large increase in radius of gyration is observed but this not accompanied by a commensurately large increase in molecular weight. (In one case, fraction G, the molecular weight actually decreases slightly.) For fractions G and H, where aromatization has been continued to ~80%, the apparent molecular weight increases to very large values.

Discussion

Degrees of Aromatization between 0 and 40%. Earlier work using size exclusion chromatography[4] on the partially aromatized polymer showed that a distinct

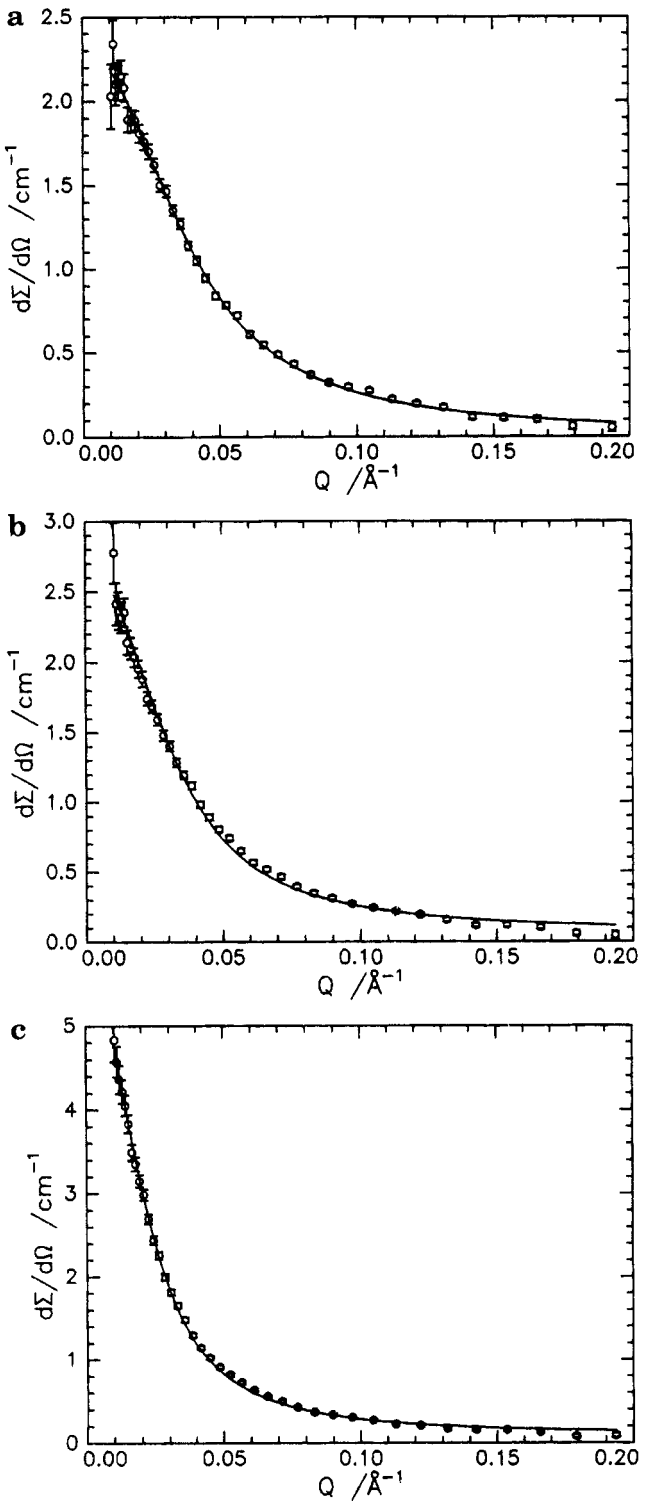

Figure 4. Fit of the Debye equation (eq 6, solid line) to the SANS data obtained for fraction D dissolved in NMP: (a) 10, (b) 20, and (c) 40% aromatization.

bimodality of molecular weight became apparent at early stages in the aromatization process. The major component of each fraction decreased in molecular weight as aromatization proceeded; at the same time the content of the second component increases in the polymer. We speculated that this behavior was caused by scission of the polymer on aromatization in the region of 1,2 linkages in the main chain and that aromatization takes place at random along the chain. The high molecular weight portion observed is due to aggregation of molecules that have a sufficiently long sequence of phenylene units, which is insoluble in the solvent.

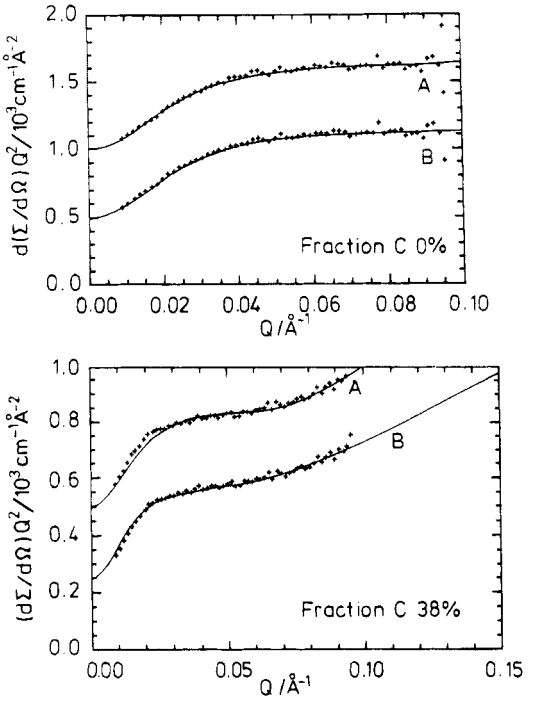

Figure 5. Fits of Yamakawa equation (eq 5; A) and Koyama equation (eq 9; B) to SANS data for fraction C for 0 and 38% aromatization. Data sets shifted away from origin for clarity.

These aggregated species are stabilized by the unaromatized poly(DHCDDMC) portions of the molecules. This model is commensurate with the changes observed in the parameters extracted from the SANS data. At low percentages of aromatization, the low molecular weight species arising from scission dominate in the specimen and consequently a reduction in molecular weight is observed. As aromatization proceeds, two effects contribute. First, as the proportion of phenylene groups in a molecule increases, a more rodlike configuration is anticipated and consequently an increase in radius of gyration ensues. Second, the proportion of aggregates in the specimen will eventually increase to such a point that their contribution to the observed scattering dominates and the apparent molecular weight should increase. Moreover, the configuration of the aggregates being radically different from the individual molecules, it is expected that this should become apparent in the observed scattering profile. In other work on dilute solutions of the hydrogenous polymer, we used the Kratky–Porod wormlike chain model to interpret intrinsic viscosity and light scattering data obtained for dilute solutions of polymers (aromatization up to 20%) in NMP. These data showed that both persistence length and shift factor increased with aromatization over this range.

We apply this model here to the SANS data. The theoretical equations obtained for the scattering law of a wormlike chain have been set out earlier. Up to ~20% aromatization good fits to the SANS data can be obtained with either of the two particle scattering functions, eqs 4 and 9. Examples of the quality of the fits are shown in Figures 5 and 6 when the data are plotted in Kratky form, i.e., $Q^2I(Q)$ as a function of Q. Table 4 gives the values of the persistence length and contour length obtained. The values of the persistence length obtained by fitting the Koyama equation to the data are generally consistently smaller than those obtained from fitting the Yamakawa expression. However, both types of fitting produce values of the contour

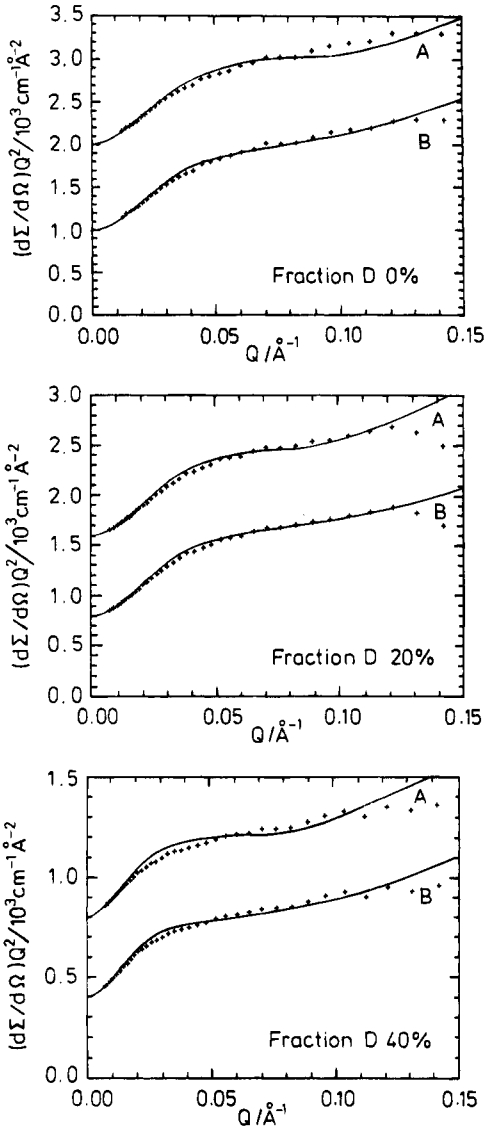

Figure 6. Fits of Yamakawa (A) and Koyama (B) equations (eqs 5 and 9, respectively) to SANS data plotted in Kratky manner for fraction D at 0, 20, and 40% aromatization. Data sets shifted away from origin for clarity.

Table 4. Persistence Lengths and Contour Lengths Obtained from SANS Data

fraction	% aromatzn	Yamakawa a/Å	Yamakawa $L/10^3$ Å	Yamakawa M_L/Å^{-1}	Koyama a/Å	Koyama $L/10^3$ Å	Koyama M_L/Å^{-1}
A	0	23	9.3	132	15	8.3	145
B	0	24	10.1	56	18	9.2	68
C	0	22	10.6	39	12	9.5	43
E	0	22	9.2	21	18	8.6	23
E	13	26	8.6	40	20	7.6	45
E	25	28	10.1	28	18	11.7	24
C	28	25	12.5	17	20	12.0	18
C	38	32	19.2	26	30	27.0	18
D	0	22	6.6	53	20	6.8	51
D	10	22	6.3		18	5.8	
D	20	26	8.1		20	7.2	
D	30	28	15.6		23	13.8	
D	40	26	15.6		24	15.6	

length that are generally in remarkable agreement with each other. The persistence lengths and the contour lengths appear to be molecular weight independent for the 0% aromatization, and assuming that this independence is maintained as the aromatization proceeds, the values in Table 4 are plotted against percentage aromatization in Figure 7. The persistence length increases as soon as aromatization begins, and the rate

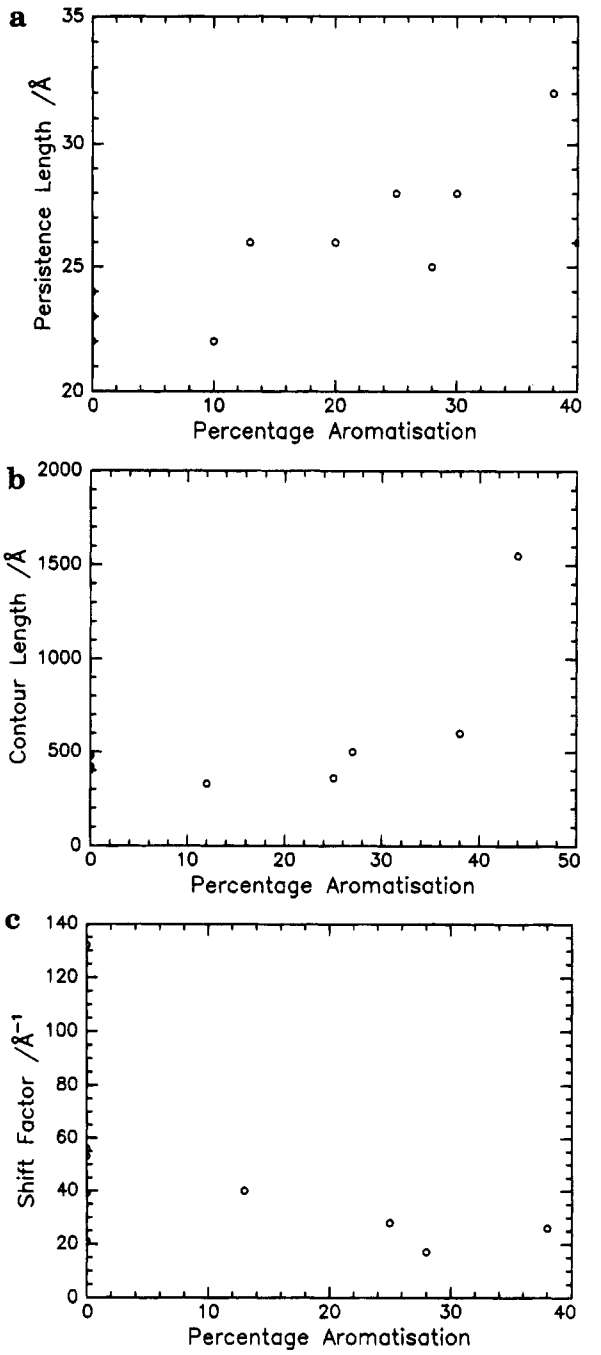

Figure 7. (a) Dependence of persistence length on percentage aromatization for all fractions. (b) Dependence of contour length on percentage aromatization for all fractions. (c) Shift factor (M_L) variation with percentage aromatization for those fractions where molecular weights are available.

of increase appears to accelerate slightly for the higher percentage aromatizations. By contrast, the contour length seems to remain almost constant as the aromatization proceeds, undergoing a rapid acceleration at the higher aromatizations.

The dependence of contour length on aromatization is complicated by the changes in molecular weight that take place on aromatization, and a more fundamental parameter to compare is the shift factor M_L ($=\bar{M}_w/L$). Where values of the weight-average molecular weight were available from the SANS data, a value of M_L has been calculated and is given in Table 4. The value of M_L should be characteristic for each polymer and depends on the trans and gauche populations of the configurational state of the polymer molecule. These

are determined by the nature of the hindrance potentials to rotation about main-chain bonds, and hence, the substituent and chemical nature of the backbone play a role in determining M_L. Consequently, while one may expect that M_L will change as the aromatization proceeds due to the loss of substituents and the change of the main chain from cyclohexyl to phenylene, one would not expect to see a variation in M_L for the precursor polymer. Our data show a large range of values for M_L for zero percentage aromatizations which appears to have a very approximate correlation with the molecular weight of the polymer. The majority of the values of the shift factor for 0% aromatization are centered around a value of 40 Å^{-1}. As the aromatization percentage increases, there is a decrease in M_L values at a slow rate to a value of ~20 Å^{-1} at 40% aromatization.

Values of persistence length and shift factor for this polymer have been obtained from light scattering and viscometry on dilute solutions for aromatizations of up to 20%. From light scattering data, M_L has a value of 26 Å^{-1} for 0% aromatization, which was reduced to 16 Å^{-1} for 20% aromatization. These values are of the same order of magnitude as reported here from SANS data. The persistence lengths obtained by light scattering range from 31 Å for 0% aromatization to 181 Å for an aromatization of 20%. Although there is considerable agreement with the SANS determined value of a at 0% aromatization, it is evident that although we do observe an increase in the persistence length from the SANS data as aromatization progresses, it is nowhere as large as that observed from the light scattering data. Although both light scattering and SANS are responding to the particle scattering function of the polymer, light scattering utilizes only the very small Q range of the particle scattering function; consequently, the light scattering data are much more responsive to the *larger* particles in the solution than SANS where we use a wide range of Q. Therefore, it is possible that the high values of the persistence length observed from the light scattering data are artifact values due to the scattered light intensity being influenced by the small amount of aggregate present in solution. For SANS, these aggregates play a much less important role because the Q range used is not sufficiently low to be influenced by their presence when SANS data are used to determine persistence lengths. The persistence lengths obtained do not appear to be significantly larger than those for common vinyl polymers[22] although larger than those quoted for polymers that have large angles between main-chain bonds (poly(dimethylsiloxane), poly(ethylene oxide)). Syndiotactic poly(vinyl chloride) has a persistence length of ~40 Å and poly(methyl methacrylate) a persistence length of 33 Å. Likewise the shift factor values obtained here are generally in the range encountered for vinyl polymers, usually between 20 and 45 Å^{-1}. Under different solvent conditions, the persistence length and shift factor can take on different values, especially the persistence length. Thus, amylose when dissolved in dimethyl sulfoxide has a persistence length of 315 Å whereas in aqueous solution a value of ~28 Å is obtained. Consequently, although the use of NMP may influence the persistence length values obtained, it does not appear that aromatization leads to any significant increase in the rodlike nature of the polymer.

Degrees of Aromatization Greater Than 40%. The changes in the scattered intensity when the aromatization exceeds 40% are very marked. Figure 8a shows the differences for one fraction at 40 and 50% aromatization. The differences are explicitly revealed when the data are plotted in Kratky plot format (Figure 8b). A definite maximum is observed at low Q for all specimens with degrees of aromatization greater than 40%. Negative deviations from the plateau behavior of Gaussian coils have often been associated with the occurrence of particular stereotactic sequences[27] along the main-chain backbone or the location of the scattering centers being at some distance from the main-chain backbone.[28] (We note here that helical wormlike chains can also lead to maximum in the Kratky plots, but these are followed by a minimum and a further increase as a increases.) None of these can be the case here since aromatization is accompanied by a loss of substituents from the cyclohexyl rings of the precursor polymer, and the formation of phenylene rings means that no stereochemical sequences are anticipated that would lead to such deviations. Formation of rodlike molecules also does not lead to the Kratky plot observed. In an earlier paper, we speculated that the high molecular weight species seen in the bimodal molecular weight distributions observed by size exclusion chromatography were due to intermolecular aggregates formed by molecules where the sequence of units that had been aromatized had exceeded a critical length. The sequences of phenylene units are insoluble in the NMP solvent, and the assembly is maintained in solution by the unaromatized chain sequences, which are solvated. Although such structures could be viewed as polymer micelles with a core formed from the aromatized units, the problem is to define a suitable model for the scattering function from which physical parameters can be extracted. The

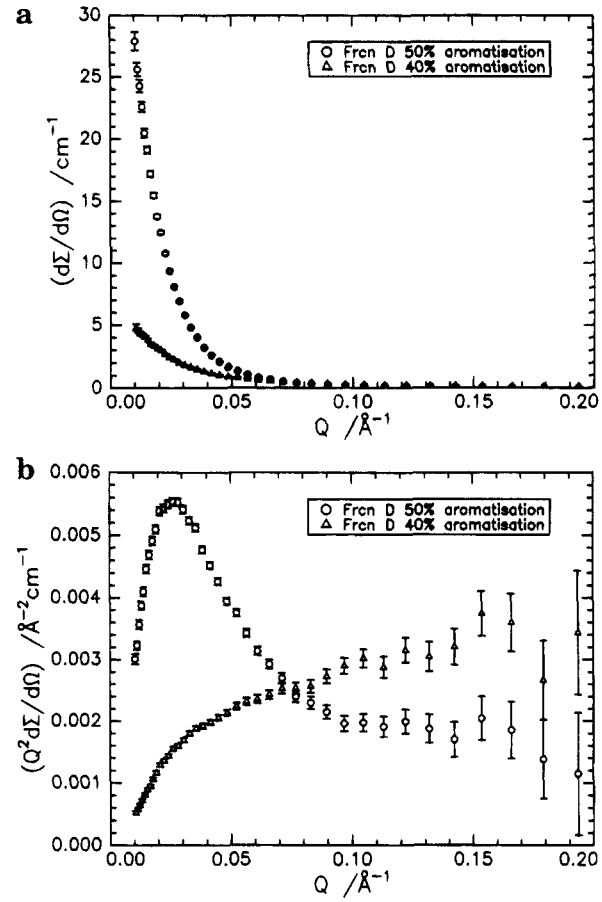

Figure 8. (a) SANS intensity as a function of Q for 40 and 50% aromatization. (b) SANS data for (a) plotted in Kratky form.

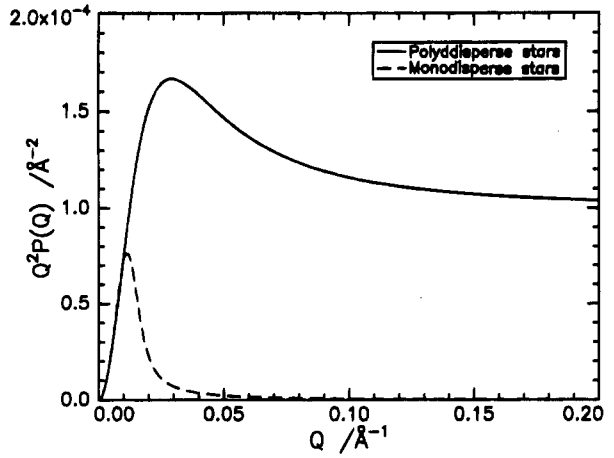

Figure 9. Kratky plots calculated for star molecules with polydisperse arms (solid line, eq 13) and monodisperse arms (dashed line, eq 13). In each case, the number of arms is 10 and the root mean square average radius of gyration is 100 Å.

model needs to have the ability to have adjustable terms which can cope with the changes consequent on aromatization. As a simple approximation, we use the notion that the aggregated entities can be viewed as ill-defined star polymers with a core formed from poly(*p*-phenylene) units and the corona being poly(DHCDDC). The particle scattering factor for regular star molecules with monodisperse Gaussian arms was derived by Benoit[29] and is

$$P(Q) = (2/fv^2)(v - (1 - \exp(-v)) + (f - 1)/2(1 - \exp(-v))^2) \quad (12)$$

where f is the number of arms on the star and v is $(f/(3f - 2))u^2$ with $u^2 = \langle s^2 \rangle Q^2$ as before. When the arms are polydisperse with a Schulz–Flory distribution, then Burchard[30] has shown that a simpler equation pertains

$$P(Q) = \frac{1 + (u^2/3f)}{[1 + u^2(f + 1)/6f]}2 \quad (13)$$

The forms of the Kratky plots obtained from these two single-particle scattering factors are shown in Figure 9. The characteristic feature is a definite peak in the Kratky plot; for a monodisperse star this is followed by a rapid decrease in the ordinate values to almost zero. Polydisperse stars retain a large finite value of the ordinate at large Q, moreover the peak is broader and the maximum shifted to a larger value of Q compared to the equivalent monodisperse star polymer. The influence of radius of gyration and arm number on the Kratky plots from such polydisperse stars is shown in Figure 10. This model has the features we desire in that the number of arms and the radius of gyration are adjustable parameters depending on the aggregation of the species. Equation 13 was fitted using nonlinear least squares to the SANS data plotted as Kratky plots for each specimen whose aromatization was 50% or greater. Typical examples of the fits are shown in Figure 11, and the radii of gyration and number of arms obtained are given in Table 5. The values given for fraction D at 80% aromatization are clearly unrealistic. The best fit of the scattering factor (Figure 12) is not good, and the maximum in the data is very broad. This broadening is probably associated with the gelation which takes place when very high percentages of aromatization are reached in solutions of poly(DHCDDC). Nonetheless, the maximum *is* still evident at approximately the same Q values as observed for the other fractions of lower percentage aromatization. We make some further remarks concerning this below. The fit to the data for this percentage aromatization and the parameters obtained are included to demonstrate that the existence of starlike structures persists into the gelation phase of the aromatization process. For fractions D and G, the change in radius of gyration on increasing the aromatization from 50 to 60% is within the error of the fitting process. All fractions show an increase in the number of arms as the aromatization increases, indicating that increased aromatization is accompanied by further aggregation to *existing* aggregates and suggests that the phenylene cores must be partially accessible. For the lowest molecular weight fraction investigated at these high percentages of aromatization (H), an increase in the radius of gyration is observed; this is accompanied by a large increase in the number of arms and hence the increase in radius of gyration is attributable to the growth of the starlike

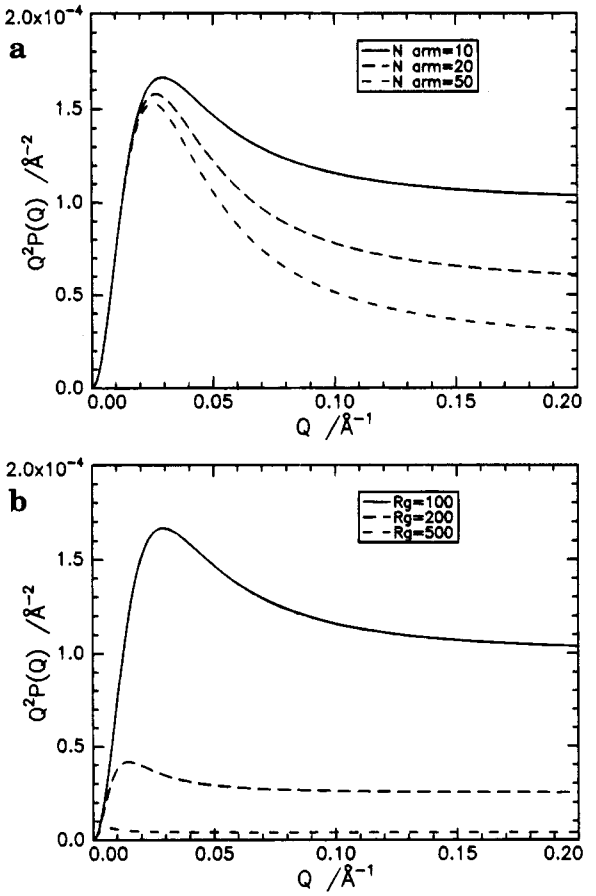

Figure 10. (a) Influence of number of arms on Kratky plot for scattering from a polydisperse star molecule with a radius of gyration of 100 Å. (b) Influence of radius of gyration on Kratky plots for polydisperse star molecules with 10 arms.

Table 5. Radii of Gyration and Number of Arms from Fitting of Polydisperse Star Model to SANS Data

fraction	% aromatzn	$\langle s^2 \rangle_z^{1/2}$/Å	n_{arm}
D	50	125	35
D	60	110	500
D	80	100	50 000
G	50	94	35
G	60	118	110
H	50	87	16
H	60	130	500

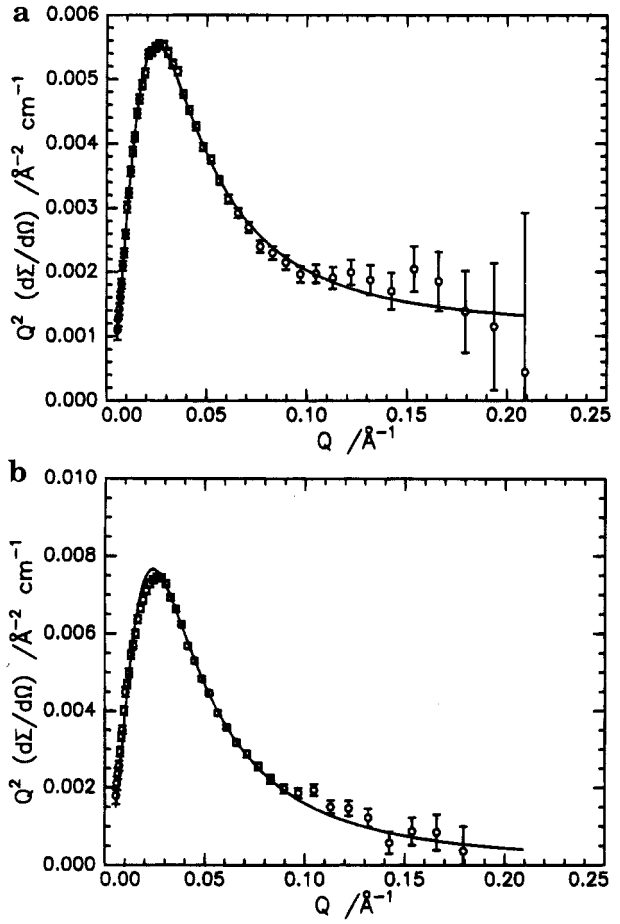

Figure 11. Fit of equation for scattering from polydisperse star molecules (eq 13) in Kratky plot form: fraction D at (a) 50% and (b) 60% aromatization.

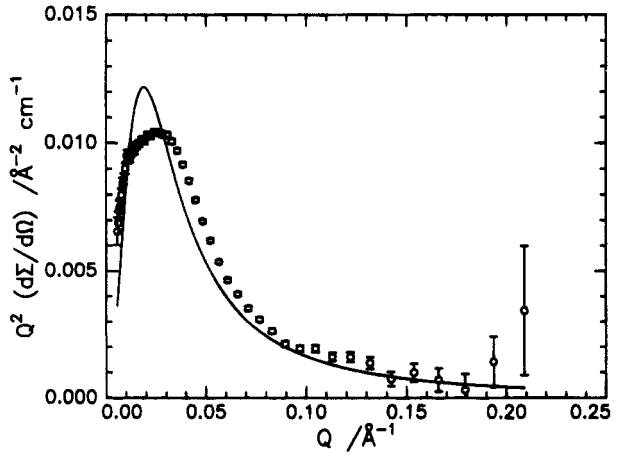

Figure 12. Best fit of eq 13, in Kratky plot form, to the scattering from fraction D at 80% aromatization.

aggregate from polymer molecules which were initially of rather low molecular weight. Although an increase in the number of arms of similar magnitude is seen for fraction D, there is no increase in radius of gyration. Since this fraction is of high molecular weight, the radius of gyration will be mainly determined by the outermost solvated parts of the poly(DHCDDC) arms and an increase in aggregation will have little influence on the radius of gyration. Aromatization of the outermost segments leads to interaggregate aromatization and the formation of a swollen gel due to solvent interaction with the remaining unaromatized segments.

This description of the structures formed is attractive since it unites the observations of aggregation at relatively low aromatization and gel formation at high aromatization. We emphasize that this is undoubtedly a simplistic description of the structural changes accompanying aromatization. For example, we have only used the very simplest particle scattering factor for stars. This only applies in very dilute solutions, and our solutions have a concentration of ~5%. For monodisperse stars, it has been demonstrated that at concentrations above the overlap value the total scattering is the product of the single particle form factor and an interference function.[31,32] The interference function has the form of a liquid structure factor due to the star molecules behaving as spheres when the number of arms is sufficiently high and leads to the observation of a maximum in the observed scattering. The structure factor for the starlike aggregates investigated here will be modified by the polydispersity of the size of the aggregates, and hence, the absence of any peak in the scattered intensity is not surprising. Furthermore, we should also bear in mind the limited Q range used here; the maximum in the scattered intensity due to any interference function contribution may be at a Q value out of the range we have investigated. Countering this argument is the observation that the position of the maximum in the Kratky plots does not change its Q value as the apparent number of arms increases. If this maximum were in any way dependent on the interference function, then as the number of arms increased, the maximum should shift to a lower Q value. This is not observed even for fraction D aromatized to 80%.

Evidently the polydisperse star model is not a valid description of the 80% aromatized fraction D. Major features of starlike scattering are retained in the Kratky plots, indicating that major aspects of starlike morphology are retained. At these high levels of aromatization, discrete starlike aggregates have become partially cross-linked together and a network structure will become more dominant as aromatization and cross-linking continues further. In the full formed network state, scattering will be dominated by correlation length fluctuations in the network. Networks have a scattering law which is proportional to $(1/(Q^2 + \xi^2))$, where ξ is the correlation length. It would appear attractive to combine the scattering laws for stars and networks together in an attempt to describe more accurately the results obtained for the 80% aromatized sample. Unfortunately such a combination in no way reproduces the observed broadening in the maximum, and when reasonable values for ξ are inserted (~20 Å) into the composite scattering law, the dependence on Q has no resemblance to the experimental data. Evidently at the highest percentage aromatization studied here the aggregate structure is considerably more complex that those we have considered here. What we have attempted is a description using the *simplest* models that can sustain the observations. We have then tried to relate the parameters of the model to the known chemistry of the aromatization process. Clearly, more complex models can always provide an apparently more complete description; however, the number of parameters increases and moreover these become interdependent on each other. Due to the increased distribution consequent on aromatization, the scattering data are insufficient to be able to discern between more complex models (such as clusters of starlike aggregates, core-shell micelles, variable density of arms in stars) and the

simple polydisperse star model we have used. We do not claim that this model is definitive of the aromatization process; we do believe that starlike entities are involved.

Conclusions

Small-angle neutron scattering studies of partially aromatized precursor polymers to poly(*p*-phenylene) have shown that for aromatizations below 40% the configuration of the molecules can be described by a wormlike chain model. The persistence length, a, increases from a value of ~22 Å for the unaromatized polymer to ~30 Å for a polymer that has been aromatized to ~40% conversion. Over this same range, the contour length increases by a larger factor. The value of the shift factor appears to be molecular weight dependent for 0% aromatization, an average value being 40 $Å^{-1}$. As aromatization increases to 40%, there is a slow decrease in the shift factor to a value of ~20 $Å^{-1}$. This range of values has also been noted from light scattering data on dilute solutions on partially aromatized polymer. Light scattering values of the persistence length of the partially aromatized polymer are larger than those obtained from SANS. This is attributable to the greater sensitivity of light scattering to the presence of aggregates which are present in small amount even when aromatization has only increased by a small extent. A stiffening of the molecule takes place on aromatization, but the consequent increase in overall dimensions is not clearly displayed due to the scission processes that accompany aromatization.

For aromatizations of 50% and greater, a distinct change in the Kratky plots is observed. These data can be reasonably well fitted using the expression for the scattering from a starlike molecule. This finding can be rationalized as due to the existence of intermolecular aggregates in the solutions, these being formed by the aggregation of long sequences of phenylene units in separate molecules. For aromatizations from 50 to 80%, the radius of gyration changes only slightly but the average number of "arms" per aggregate increases markedly, although we believe that simple star model is invalid for the 80% aromatized material. As for the well-characterized monodisperse stars, it is believed that it is the outermost regions of the solvated poly(DHCDDMC) arms which determine the radius of gyration, and thus as long as these are not aromatized, the radius of gyration changes but little. When these outer regions aromatize, interaggregate links are formed which lead to the gelation observed at high aromatizations. The polydisperse star model employed here is the simplest that supports the observations. We do not claim it is a definitive model for all stages of the aromatization, but starlike formations certainly participate.

Acknowledgment. J.R.H. thanks the SERC for the provision of a maintenance grant and ICI plc for contributions during the course of this work. R.W.R. and J.R.H. thank ICI plc for the provision of the deuterated monomer and the SERC (now EPSRC) for supporting neutron beam facilities at Institut Laue-Langevin, Grenoble, and ISIS at the Rutherford Appleton Laboratory.

References and Notes

(1) Leising, G. In *Intrinsically Conducting Polymers: An Emerging Technology*; Aldissi, M., Ed.; NATO ASI Series E; Applied Sciences, Reidel: Dordrecht, The Netherlands, 1993; Vol. 246.
(2) Grem, G.; Leditzky, G.; Ullrich, B.; Leising, G. *Adv. Mater.* **1988**, *4*, 36.
(3) Grem, G.; Leditzky, G.; Ullrich, B.; Leising, G. *Synth. Met.* **1992**, *51*, 383.
(4) Holland, J. R.; Richards, R. W.; Burgess, A. N.; Nevin, A. *Polymer* **1994**, *35*, 4133.
(5) Ballard, D. G. H.; Courtis, A.; Shirley, I. M.; Taylor, S. C. *Macromolecules* **1988**, *21*, 294.
(6) Conticello, V. P.; Gin, D. L.; Grubbs, R. H. *J. Am. Chem. Soc.* **1992**, *114*, 3167.
(7) Holland, J. R.; Richards, R. W.; Burgess, A. N.; Nevin, A. *Polymer*, in press.
(8) Kratky, O.; Porod, G. *Recl. Trav. Chim. Pays Bos. Belg.* **1990**, *68*, 1106.
(9) Mattice, W. L.; Suter, U. W. *Conformational Theory of Large Molecules*; Wiley Interscience: New York, 1994.
(10) Benoit, H.; Doty, P. *J. Phys. Chem.* **1953**, *57*, 958.
(11) Neugebauer, T. *Ann. Phys.* **1943**, *42*, 509.
(12) Heine, S.; Kratky, O.; Roppert, R. *Makromol. Chem.* **1962**, *56*, 150.
(13) Kirste, R. G. *Makromol. Chem.* **1967**, *101*, 91.
(14) Daniels, H. E. *Proc. R. Soc. Edinburgh* **1952**, *63*, 290.
(15) Hermans, J. J.; Ullman, R. *Physica* **1952**, *18*, 951.
(16) Burchard, W.; Kajiwara, K. *Proc. R. Soc., A* **1970**, *316*, 185.
(17) Yamakawa, H.; Fujii, M. *J. Chem. Phys.* **1976**, *64*, 5222.
(18) Yamakawa, H.; Fujii, M.; Shimada, J. *J. Chem. Phys.* **1976**, *65*, 2371.
(19) Fujii, M.; Yamakawa, H. *J. Chem. Phys.* **1977**, *66*, 2578.
(20) Yamakawa, H.; Fujii, M. *J. Chem. Phys.* **1977**, *66*, 2584.
(21) Yoshizaki, T.; Yamakawa, H. *Macromolecules* **1980**, *13*, 1518.
(22) Yamakawa, H. *Annu. Rev. Phys. Chem.* **1984**, *35*, 23.
(23) Debye, P. *J. Phys. Colloid. Chem.* **1947**, *51*, 18.
(24) Koyama, S. *J. Phys. Soc. Jpn.* **1973**, *34*, 1029.
(25) Kurata, M.; Stockmayer, W. H. *Fortschr. Hochpolym. Forsch.* **1963**, *3*, 196.
(26) Ullman, R. *J. Polym. Sci., Polym. Lett.* **1983**, *21*, 521.
(27) Hopkinson, I.; Kiff, F. T.; King, S. M.; Munro, H.; Richards, R. W. *Polymer* **1994**, *35*, 1722.
(28) Rawiso, M.; Duplessix, R.; Picot, C. *Macromolecules* **1987**, *20*, 630.
(29) Benoit, H. *J. Polym. Sci.* **1953**, *11*, 507.
(30) Burchard, W. *Macromolecules* **1977**, *10*, 919.
(31) Dozier, W. M.; Huang, J. S.; Fetters, L. J. *Macromolecules* **1991**, *24*, 2810.
(32) Willner, L.; Jucknischke, O.; Richter, D.; Roovers, J.; Zhou, L.-L.; Toporowski, P. M.; Fetters, L. J.; Huang, J. S.; Lin, M. Y.; Hadjichristidis, N. *Macromolecules* **1994**, *27*, 3821.

MA950434S